Analytical Model for Effects of Twisting on Litz-Wire Losses

Charles R. Sullivan
Thayer School of Engineering at Dartmouth
14 Engineering Drive, Hanover, NH 03755, USA
Email: charles.r.sullivan@dartmouth.edu

Richard Y. Zhang
Dept. Elec. Eng. & Comp. Sci., M.I.T.
Cambridge, MA, USA
Email: ryz@mit.edu

***Abstract*—Litz wire uses complex twisting to balance currents between strands. Most models are not helpful for choosing the twisting configuration because they assume that the twisting works perfectly. A complete model that shows the effect of twisting on loss is introduced. The model can predict loss for a precise configuration, but in practice, it is difficult to achieve sufficient manufacturing precision to use this approach. More practically, the model can predict worst-case loss over the range of expected production variation. The model is useful for making design choices for the twisting configuration and the pitch of the twisting at each level of construction.**

I. Introduction

Litz wire uses complex twisting configurations to balance currents between strands. Most models, including [1]–[10], assume that this twisting works perfectly and in fact the current is equal in every strand. In many cases, this is a good assumption, but there are practical cases in which the details of the twisting configuration make the difference between good performance and excessive losses. In order to make good design choices for the details of construction, including the number of strands combined in each construction operation, and the pitch and direction of twisting in each operation, it is necessary to model the effects these details have on the power losses. Recent work has experimentally [11], [12] and numerically [13] demonstrated that not all litz constructions behave the same, confirming the need for a model that takes the construction details into account.

We introduce here the first complete analytical model for litz wire that shows the effects of twisting on loss. This is accomplished by modeling four types of frequency-dependent loss effects: skin-effect and proximity effect, each at the strand level and at the bundle level. For wires that are constructed in multiple successive twisting operations, the bundle level effects are analyzed for each level of construction. Well known models are used for the strand-level effects, and are extended to also address bundle-level effects. The pitch of twisting at each level affects the bundle diameter, the dc resistance, and the bundle-level proximity effect, and each of these effects is modeled in order to enable examining the tradeoffs in the choice of pitch.

This paper has twin goals. The immediate goal is an academic goal to develop a complete model of litz wire, in order to resolve questions about how it works, and about when different loss effects are and are not important. The model allows answering these questions for any litz-wire construction in any transformer or inductor winding application. The ultimate goal is a practical goal, to verify existing design guidelines, such as those provided in [12], and to extend them to provide guidance on all aspects of litz-wire design. In particular, many design methods provide guidance on the number and diameter of strands to use. The method in [12] is particularly recommended because it provides a simple-to-use method that takes into account trade-offs between cost and loss in choosing the number and diameter of strands. Also provided in [12] is a simple and systematic method for choosing some of the construction details— the number of strands to be combined in each twisting operation. However, it does not provide guidance on the pitch or direction of twisting, and in practice these choices are made based by manufacturers based on experience. Typical choices for these parameters may be related more to ease of construction than electromagnetic effectiveness.

With the model presented here, it is possible to analyze a particular transformer or inductor configuration and to comprehensively predict litz-wire loss effects for a complex litz-wire construction with hundreds or thousands of strands using only milliseconds of computation time on a personal computer. This allows evaluating a wide range of construction details in order to find good design choices. However, the calculations are conceptually complex even though they are computationally efficient, and the ultimate goal, not yet fully realized here, is to provide simple rules for choosing effective twisting pitches, in the same spirit as the simple guidance provided for other design aspects in [12].

II. Nomenclature

In the field of wire rope, *wire* means an individual fine solid wire; many of these wires are twisted together to form a *strand*; and finally a set of strands is twisted together to form a wire rope.

In the field of litz wire, end result of all the twisting construction steps is called a *litz wire*. The individual fine solid wires are insulated before the first twisting operation and are properly called *magnet wires*. However, in the field of litz-wire applications, the magnet wires used as a starting point for litz construction are usually called *strands*, a different terminology from what is used in the wire rope field. That is

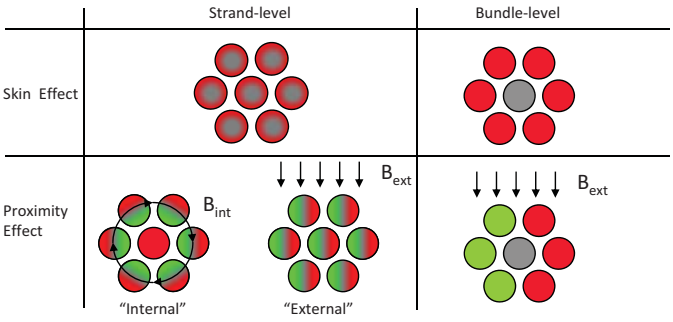

Fig. 1. Conceptual illustration of the types of eddy-current loss in litz wire. Note that the current distributions shown are not realistic for the wire construction shown, but instead show what would hypothetically happen if only the effect being illustrated were in effect and the others were magically turned off.

the terminology used here. Given that the term *strand* is no longer available to mean a twisted group of magnet wires at an intermediate level of the construction, the term *bundle* will be used for a twisted group of wires or *sub-bundles*.

Losses in litz wire can be classified into resistive loss ($I_{rms}^2 R_{dc}$) and eddy-current losses, which can be further classified into skin effect and proximity effect, each of which can occur at the level of the individual strand or at the level of each bundle or sub-bundle, as diagramed in Fig. 1. Skin effect as the tendency for high-frequency currents to flow on the surface of a conductor. At the strand level, that means the tendency to flow on the surface of each strand; at the bundle level it means the tendency to flow preferentially in the strands at the surface of the bundle. We define skin effect loss as inclusive of resistive loss:

$$P_s = F R_{dc} I_{rms}^2 \tag{1}$$

where F is a skin-effect factor, R_{dc} is the dc resistance, and I_{rms} is the current in the wire.

Proximity effect is eddy current that results from an ac magnetic field imposed on a conductor. The term *proximity effect* originated because a nearby ac-current-carrying conductor creates such a field. The effect is driven by the total magnetic field, which is a result of the configuration of all the current-carrying conductors and magnetic materials in the region, and is best understood as a result of an externally imposed magnetic field, not directly as a result of distances between conductors. As with skin effect, it can be divided into strand-level and bundle-level effects, as shown in Fig. 1. In some ways of describing litz wire, strand-level proximity effect loss $P_{p,0}$ is separated into "internal" and "external" components, due to the field generated by current in the other strands in a given turn of a litz wire winding, and the field generated by other turns. As will be shown in Section IV, it is more straightforward to consider these two components together for our analysis; in each proximity effect calculation, $\hat{H}$ is the total field, not just the external field.

We quantify proximity effect losses in terms of a proximity-effect factor G defined by

$$P_p = G \hat{H}^2 \ell \tag{2}$$

where $\hat{H}$ is the peak magnitude of a sinusoidally varying magnetic field $H(t)$ and ℓ is the length of the wire. This is computed as the sum of the effects at the individual strand level,

$$P_{p,0} = G_0 \hat{H}^2 \ell \tag{3}$$

and at the level of each successively constructed bundle:

$$P_{p,i} = G_i \hat{H}^2 \ell \tag{4}$$

where $i = 1$ is the first twisting operation that combines simple magnet wires (strands) into a twisted bundle, and the largest value of i corresponds to the final twisting operation that results in the finished litz wire.

Note that a measurement or simulation of the resistance of a single litz wire, not in a winding or otherwise subjected to an external field, includes internal proximity effect losses, and a "black box" description of the behavior of that wire would describe all the loss that occurs in that scenario as skin effect loss reflected in an overall F value, as in [13]. Thus, a calculation this overall F value would require knowing G_i for $i = 0$ to one less than the number of levels of construction used. In this paper, however, we define F based on the origin of the loss rather than based on black-box behavior, and so we do not include the internal proximity effect losses in F. The internal proximity effect losses are included instead in the G values.

Some geometrical parameters to be used in the analysis are:

- d_0 is the diameter of a strand; d_i is the diameter of a bundle completed in twisting step i.
- Likewise, $r_i = d_i/2$.
- p_i is the pitch for the i^{th} twisting operation—the axial distance over which the twisting completes a full rotation.

III. Skin Effect and Dc Resistance

The strand-level skin-effect factor F_0 is given by the standard Bessel-function solution [10].

$$F_0 = \Re\left(\frac{\rho \ell}{2\pi r^2} j^{\frac{3}{2}} \xi \frac{J_0\left(j^{\frac{3}{2}}\xi\right)}{J_1\left(j^{\frac{3}{2}}\xi\right)} \right) \tag{5}$$

where

$$\xi = \frac{\sqrt{2}}{\delta} r \tag{6}$$

and J_0 and J_1 are Bessel functions of the first kind of order 0 and 1, respectively; ρ is the conductor resistivity; and the electromagnetic skin depth is $\delta = \sqrt{\frac{\rho}{\pi \mu_0 f}}$, where μ_0 is the permeability of free space ($4 \cdot 10^{-7} \cdot \pi$ H/m) and f is the frequency at which the losses are to be analyzed.

R_{dc} is affected by the increase in length caused by twisting. In an ideal litz wire, all the strands circulate between all possible positions in the bundle, and all are the same length (if the wire is sufficiently long compared to the pitches for

the position rotation to average out well). This is achieved if each twisting operation combines no more than 5 strands or sub-bundles [12]. In such a case, we can calculate the length of one strand explicitly and then use that same length for all the strands. The position in the cross section (the $x-y$ plane) in terms of the position along the length of the wire (z) is given by

$$x(z) = \sum_i r_{c,i} \cos(k_i z) \tag{7}$$

$$y(z) = \sum_i r_{c,i} \sin(k_i z) \tag{8}$$

$$\tag{9}$$

where $r_{c,i}$ is the radius from the center of the bundle created in twisting step i to the centers of the sub-bundles that are being twisted together, and $k_i = 2\pi/r_i$. The length of the strand is found by numerically integrating along the length,

$$\ell_s = \int_0^\ell \sqrt{\left(\left(\frac{dx}{dz}\right)^2 + \left(\frac{dy}{dz}\right)^2 + 1\right)} dz \tag{10}$$

If a large number of strands is combined in one operation (7 or more), the lengths are not all the same, and an average length can be used instead. Assuming that the position of the strand in a simply twisted bundle is a continuous variable, and averaging the length over the area of the bundle cross section, we find that the average length of strands in a simply twisted bundle of many strands is increased over the dc resistance by a factor

$$\frac{R_{dc,twisted}}{R_{dc,untwisted}} = \frac{\left(\frac{p^{\frac{4}{3}}}{r^{\frac{4}{3}}} + 4\pi^2 \frac{r^{\frac{2}{3}}}{p^{\frac{2}{3}}}\right) - \frac{p^2}{r^2}}{6\pi^2} \tag{11}$$

where r is the outer radius of the bundle, which is itself a function of the twisting pitch. The bundle radii can be estimated as discussed in Section V, or directly measured on a sample. For practical pitch-to-radius ratios (between 2 and 100), the result in (11) can be reproduced with less than 0.25% error by calculating the length of a helical path of the same pitch at a radius $r_c = 0.6928r$. In other words, the weighted average radius of a strand path can be considered to be 69.28% of the radius of the bundle. This approximation allows treating large numbers of strands combined in one twisting operation under the same framework and calculating the length with (7) and (10) to allow addressing multiple levels of twisting for any number of strands. For numbers of strands up to 6, the radii are identical for each strand or sub-bundle and r_c in (7) can be the actual parameter calculated based on the geometry; for higher numbers of strands $r_c = 0.6928r$ is used.

The skin effect factor for each successive level beyond the strand level ($F_{i>0}$) can be simply approximated by using an average conductivity and the overall bundle diameter in the same skin effect calculation. The average conductivity is the conductivity of the conductor material (e.g. copper at the temperature of operation) scaled by two factors. First it is scaled by the density of conductor packing in the bundle, and second it is scaled by the inverse of the increase in length caused by twisting. Note that the effective conductivity is different at different levels of construction, as the overall packing density decreases at each construction step. Using an effective conductivity works well for tightly packed strands, which is typically the case for litz wire. For strands that are more widely spaced, the approximations is less accurate because it neglects the local field energy that occurs when the current is concentrated into fine strands. Thus, the actual bundle-level skin effect is not as severe as this would predict, so this estimate is conservative in the extreme cases of wide strand spacing, but is accurate for typical litz wire.

The total skin effect loss is given by

$$P_s = R_{dc} I_{rms}^2 F_0 F_1 F_2 ... \tag{12}$$

As noted above, this loss is the total loss incurred by the skin effects occurring at each level, but it is not the total loss in an isolated wire, which would additionally have internal proximity effect losses.

IV. Proximity Effect

Proximity effect eddy currents are in a direction to oppose the applied field. In the extreme of large eddy currents, the field can be significantly reduced. Because such a "self-shielding" effect only occurs with large eddy currents, self-shielding will not be important in typical good designs. Thus, we proceed to analyze proximity effect assuming the self-shielding effect is small.

A. Strand level

With no self-shielding, for uniform field $\hat{H}$, the loss in a single strand is [14], [15]

$$P_{p,0} = \frac{\pi \ell d_0^4 \omega^2 \mu_0^2 \hat{H}^2}{128\rho} \tag{13}$$

where ℓ is the length of the strand, which is on average longer than the length of the bundle because of twisting. Based on (13), the strand level proximity effect is factor is given by

$$G_0 = \frac{\pi d_0^4 \omega^2 \mu_0^2}{128\rho} \tag{14}$$

Now consider nonuniform $\hat{H}$. For a small strand, $\hat{H}$ is unlikely to vary significantly over the cross section, so we can consider it to be only a function of z, a coordinate along the length of the strand, curving to following the strand around a winding, for example. $\hat{H}(z)$ in general has three components, in x, y and z directions, but we neglect the z component because typical winding designs have no significant field in that direction, and even if they did, the proximity effect induced by such a field would be small.

In a given section of the strand along the length, the loss induced depends only on the magnitude of $\hat{H}$ in the xy plane, $|\hat{H}(z)| = \sqrt{\hat{H}_x^2(z) + \hat{H}_y^2(z)}$, not on its direction. And the total loss is given by

$$P_{p,0} = nG_0 \int_0^\ell |\hat{H}(z)|^2 dz \tag{15}$$

assuming that the integral along the length is the same for each strand. (If it's not the same, the individual integrals can be taken instead of multiplying by the total number of strands, n.) Equivalently, we can use the rms average of $|\hat{H}(z)|$ along its length in $P_{p,0} = nG_0\hat{H}^2\ell$. Note that $\hat{H}$ is the total field, including internal and external field. A given strand will experience the same loss when subjected to a given field strength, regardless of the origin of that field.

The field in a winding can be estimated by simulating or analyzing the whole winding as a region of uniform current density. Given the results of such a simulation, it is simpler to compute the rms average of $|\hat{H}|$ over the volume of the winding rather than along the wire path. The result of such an average is actually more accurate than using (15) because it avoids using the path of one strand as representative of the full bundle.

B. Bundle level

First we consider an untwisted bundle–a cylindrical bundle of straight strands, connected together at the ends. In a uniform field, the proximity effect behavior is essentially the same as a solid wire with same outside diameter and a conductivity equal to the average conductivity of the bundle, resulting in an effective resistivity $\rho_{\mathrm{eff},1}$, where the subscript 1 indicates a value for the first level of construction. so (13) becomes

$$P_{p,1,\mathrm{untwisted}} = \frac{\pi\ell d_1^4\omega^2\mu_0^2\hat{H}^2}{128\rho_{\mathrm{eff},1}} \tag{16}$$

and we define

$$G_1 = \frac{\pi d_1^4\omega^2\mu_0^2}{128\rho_{\mathrm{eff},1}} \tag{17}$$

However, when we consider a nonuniform field, the behavior diverges from the strand-level behavior. We can no longer consider the local loss to be a result of the local field strength, independent of direction. Instead, the current must flow in a loop around the whole length, so it's the net flux linked for full length of the wire that matters.

For a case including variation along z of the field strength and direction, but still untwisted, we obtain

$$P_{p,1,\mathrm{untwisted}} = \frac{G_1}{\ell}\left(\left(\int_0^\ell \hat{H}_x(z)dz\right)^2 + \left(\int_0^\ell \hat{H}_y(z)dz\right)^2\right) \tag{18}$$

This has an important difference relative to (15) in that integral is performed *before* the vector magnitude is taken and squared. This means that the effect of a field in one direction in one region can be canceled by a field in the opposite direction in another region. This potential for cancelation is the reason it is possible to drastically reduce proximity effect with properly constructed litz wire.

Now consider twisting. This affects strand length and bundle diameter so the diameter and the effective resistivity are adjusted for that as before. But more interesting is is effect on bundle level proximity effect. This can be addressed simply by using local coordinates twisting with the bundle to re-write $\hat{H}_x(z)$ and $\hat{H}_y(z)$ for the calculation in (18). Adding a coordinate rotation along the length results in

$$\begin{aligned} P_{p,1} =& \frac{G_1}{\ell}\left(\int_0^\ell \Big(\cos(kz)\hat{H}_x(z) + \sin(kz)\hat{H}_y(z)\Big)\,dz\right)^2 \\ &+ \frac{G_1}{\ell}\left(\int_0^\ell \Big(\cos(kz)\hat{H}_y(z) + \sin(kz)\hat{H}_x(z)\Big)\,dz\right)^2 \end{aligned} \tag{19}$$

For strand-level proximity effect, the integral along the length of the bundle was a poor approximation of the integral. For example if there is a linear gradient of field strength across the bundle in the x direction, using the field in the center of the bundle as representative would be in effect using the simple average instead of the rms value. We saw that it was better to use the volume rms average of the field over the whole volume. This avoids the systematic error that would result from using the center-of-bundle value. However, for bundle-level effects, using the the center-of-bundle value as in (19) does not incur any error when there is a linear gradient, because again it is the total flux linked that produces the total current flow.

For a multi-level construction, the same calculation can be performed for each value of i. In summing the losses, note that the loss calculated for a given bundle needs to be multiplied by the total number of those bundles. At this point, the value of using the total field rather than separating the external and internal field becomes clear–the accounting necessary to keep track of which fields count as external and internal for each level would be become complex, and it is unnecessary. For a twisted sub-bundle following a helical path, the twist rate used for the coordinate rotation in (19) is ordinarily the rotation relative to the global coordinate system of the litz wire, not the local coordinates that follow the twisting bundle. The field must also be in the global coordinates, as is obtained from a simulation of the overall field representing the winding as a large region of uniform current density. An exception to this is if the wire is not wound in a winding, but is simply used as an isolated conductor, or as the center conductor of a coaxial cable. In such cases the field of interest would be only the internal field, which would be more easily represented in local coordinates as the sub-bundle twists around the overall bundle.

The accuracy of this method is expected to be very good with the following caveats. One is that the diameter of the bundle is an important parameter, and so the accuracy of the bundle diameter estimate used will affect the accuracy of the result. Another is that, as shown in the examples that follow and in [13], small changes in pitch can result in large changes in bundle-level proximity effect loss, because of periodic nulling of the net flux. Thus, specific predictions are less valuable than scans over a range of values which can predict worst case for manufacturing variations. As noted before, we are assuming that bundle-level effects are small enough that the self-shielding effect is small–that will be true in good

designs, but bad designs may not be as bad as the calculation predicts. Finally, we note that a minor approximation is that one effective conductivity characterizes the whole diameter of a bundle created at one level of construction. For large number of strands combined in one operation with a tight twisting pitch, the strands at the outer diameter will be significantly longer than strands at the center, and thus the outer region has a higher effective resistivity. Using the average length for the effective resistivity is not quite correct because the outer strands link more flux and are more important for the bundle-level proximity effect losses.

V. Implementation

The calculations in Sections III and IV have been implemented in a set of MATLAB functions, taking as inputs

- The number of strands or sub-bundles to be combined at each step.
- The pitch for each of these operations.
- The bare strand diameter, insulated strand diameter, and an packing factor to account for density of packing of strands and bundles.
- The length of the overall litz wire.
- The H field to which the wire is subjected, specified as an RMS value over the whole winding region used for calculating strand-level proximity effect $P_{p,0}$ and as an array of H values along the length of the wire used for calculating bundle-level proximity effects $P_{p,i}$.
- The conductor resistivity.
- The frequency and rms value of the current in the wire.

The diameters of the bundles are calculated based on the optimum results for circle packing in [16], optionally scaled based on the packing factor. The results are then adjusted for twisting by assuming that the outer strands or sub-bundles in a bundle form a circle and that this configuration stays constant as the paths of the strands are twisted into helical paths. This calculation is accurate for numbers of strands up to 7 and for some other particular number os strands, but is a worst-case estimate for others. It is assumed that sub-bundles do not deform when they are twisted into higher-level bundles. In practice, such deformation is significant, especially when the sub-bundle is not tightly twisted (i.e., when the sub-bundle has a large pitch) and when the directions of subsequent twisting operations are the same.

The necessary H-field data can be simply calculated for a transformer geometry based on the assumption of a field strength that varies linearly from zero to $\hat{H}_{max} = NI/b$ where b is the breadth of the core window. This results in a value of $\hat{H}_{rms} = NI/(b\sqrt{3})$. Values along the center of the wire for layer m of an M-layer winding are $\hat{H}_m = \hat{H}_{max}(m-0.5)/M$.

For situations with more complex fields, such as gapped inductors, various options are possible for calculating the H-field data, including using a magnetostatic finite-element analysis, as was done for the inductor example discussed in Section VII-A.

VI. Numerical Verification

The results of the implementation described in Section V were benchmarked against a custom build of the FastLitz three dimensional (3-D) numerical litz analysis software [13] developed for this purpose. The examples simulated for the benchmarking were chosen to exercise the models over a range of different construction types and excitations, and for numerical feasibility, not to be representative of real applications. Example applications are discussed in Section VII. The litz wires tested each use a total count of 125 strands, 0.1 mm diameter, with 0.11 mm outside diameter including insulation, and were constructed as 125 simply twisted strands, 5 bundles of 25 strands each (5×25), 25 bundles of 5 strands each (25×5), and 5 bundles of 5 bundles of 5 strands each (5×5×5), with various pitches.

The first test was bundle-level skin effect. A 35 mm long section was analyzed and simulated with the new model and with FastLitz. For the simply twisted construction, a two-dimensional (2-D) simulation can also be used. The 2-D simulation cannot capture the twisting effects, but the twisting is not expected to significantly affect the results in this case. The results are summarized in Fig. 2, showing excellent agreement between the different models, both in terms of the effect of construction and the quantitative results. The average absolute value of the percentage error between the new model and FastLitz is 2.3% and the maximum 3.6%, well within the expected error of the numerical approach taken in FastLitz.

The differences between the performance of the different constructions are as expected based on the model and the discussion in [12]. The 5×5×5 yields no bundle level skin effect, and the predictions of the two models agree. Both models also predict very little skin-effect resistance for the 5×25 construction, and higher resistance for the 25×5 construction. That is also as expected. The final step of twisting has the largest potential for skin effect because it is where the diameter is largest compared to skin depth, and combining 25 sub-bundles in that step leaves some buried in the inside where they carry less current, whereas combing 5 bundles in that step prevents any skin effect at that level. In fact, the 25×5 construction has essentially the same skin-effect resistance as the simply twisted 125-strand bundle. The multi-level construction only provides significant benefits if the higher-level twisting steps combine 5 or fewer sub-bundles.

Fig. 3 shows the 2-D simulation of the same 125-strand packing configuration that was assumed in FastLitz. The non-circular bundle shape leads to some current crowding in the protruding strands around the perimeter. However, the extra loss that results from these do not seem to be significant, and the ac-to-dc resistance ratio from this simulation matches the prediction of the new model, based on a circular bundle shape, within less than 0.5%.

Bundle-level proximity effect was tested with a 20 mm long section of litz wire, with all the strands shorted together at each end, subjected to a uniform 10-kHz sinusoidally varying H field with peak magnitude $\hat{H} = 10$ kA/m. The constructions

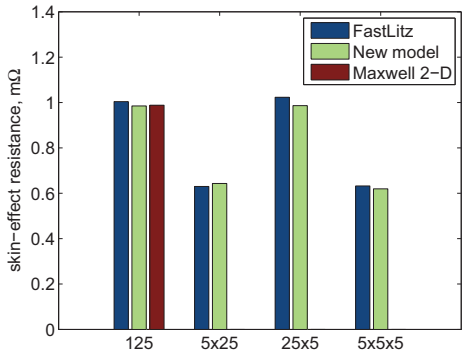

Fig. 2. Bundle-level skin-effect resistance predicted by the model described here compared to results from a FastLitz [13] simulation for three different constructions, 125 simply twisted strands, 5 bundles of 25 strands each (5×25), 25 bundles of 5 strands each (25×5), and 5 bundles of 5 bundles of 5 strands each (5×5×5). For the simply twisted bundle, an ANSYS Maxwell 2-D simulation result is also included. The twisting pitches were 50 mm for the single-step 125 strand construction, 20 mm for the first level and 50 mm for the second level in the 5×25 and 25×5 constructions, and 10, 20, and 50 mm for the three successive twisting steps in the 5×5×5 construction. All pitches are reported as the final configuration in global coordinates. Alternate layers used alternate twisting directions.

tested were simply twisted 125 strands, 5×25 and 25×5. The pitch of the final twisting operation was swept over a range from 10 mm to 100 mm. For the 5×25 and 25×5 constructions, the first level was twisted with 20 mm pitch. Figs. 4, 5, and 6 show the results for the new model (curves) and for FastLitz (points). Both methods predict the same type of behavior with respect to pitch. FastLitz predictions are consistently about 15% to 25% lower than predictions of the new method. This small discrepancy may be due to minor differences in the geometry modeled in the two methods. It is possible to obtain a nearly exact match between the methods by varying the packing factor parameters. The plots were generated using identical nominal values for insulation thickness and packing density without attempting to match the

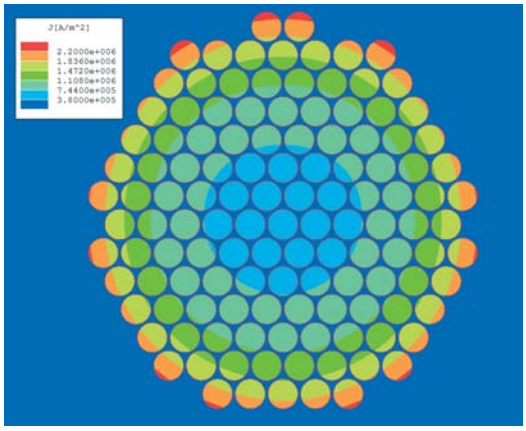

Fig. 3. A 2-D simulation of a 1-A, 100-kHz total current in the 125-strand configuration used of skin-effect verification, with shading to indicate current density.

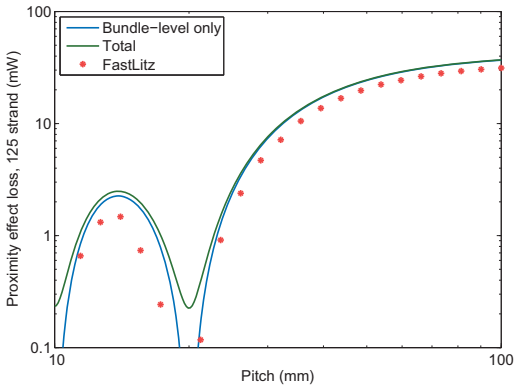

Fig. 4. Proximity effect losses for a simply-twisted bundle of 125 0.1 mm strands subjected to a uniform 10-kHz sinusoidally varying H field with peak magnitude $\hat{H} = 10$ kA/m as a function of pitch, as predicted by the new model and by FastLitz [13].

mechanical or electromagnetic results.

Note that the bundle-level proximity effect for the different constructions is nearly identical, with the only significant difference being slightly lower loss for the simply twisted 125-strand construction. That is a result of the smaller overall diameter achieved in that simpler construction. As discussed in [12], the choice of the number of levels of construction is important for bundle-level skin effect but not bundle-level proximity effect.

Overall, the verification has confirmed that the new model is highly accurate. Comparisons with numerical models show average error of 2% for skin effect, error that is likely to be mostly the inherent tolerance in the numerical results. Comparison of bundle-level proximity effect show average error around 20%. We believe this larger error is due to the fact the the detailed geometry of the bundle is more important for bundle level proximity effect. A closer match between

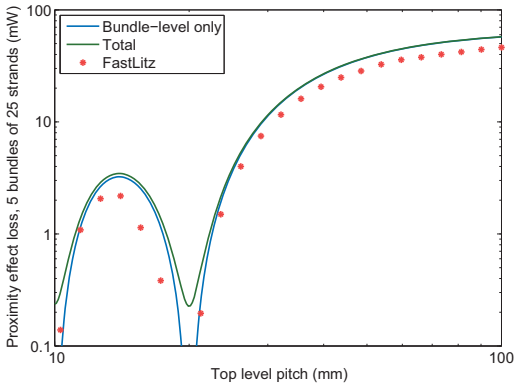

Fig. 5. Proximity effect losses for a wire consisting of 5 sub-bundles, each having 25 strands of 0.1 mm magnet wire (5×25 construction), subjected to a uniform 10-kHz sinusoidally varying H field with peak magnitude $\hat{H} = 10$ kA/m, as a function of pitch for the final twisting operation, as predicted by the new model and by FastLitz [13].

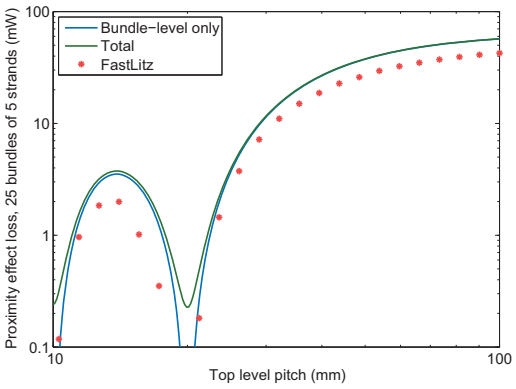

Fig. 6. Proximity effect losses for a wire consisting of 25 sub-bundles, each having 5 strands of 0.1 mm magnet wire (25×5 construction), subjected to a uniform 10-kHz sinusoidally varying H field with peak magnitude $\hat{H} = 10$ kA/m, as a function of pitch for the final twisting operation, as predicted by the new model and by FastLitz [13].

the different analysis methods could be obtained by ensuring that they assume exactly the same geometry. The accuracy in practice is expected to be limited primarily by our ability to match the geometry used in the analysis to the geometry of a manufactured litz wire.

As expected for an analytical model, the new method is orders of magntidue faster to compute than a numerical model, even though we perform the simple integrals (10) and (19) numerically. For example, the 5×5×5 construction (which is the most complex of these examples for the new model to analyze), a full analysis of skin and proximity effect at the strand level and all bundle levels takes less than 15 milliseconds, whereas FastLitz takes 10 seconds just to analyze the bundle-level effects, using the same computer. The fast computation of the analytical method is useful in facilitating optimization and in examining the impact of variations in geometry, as are expected in practical manufacturing.

VII. Design

For a typical transformer, the bundle-level proximity effect will be caused by a field that is roughly constant in each layer of the winding, so the field to be integrated is a staircase function with as many steps as there are winding layers. The length of each step is different because the turn lengths are different in each layer. The loss can be nulled by having an integer number of twists in each layer, or can be nulled globally without meeting that condition, in some cases using an overall non-integer number of twists.

However, that nulled solution is not of practical value. It implies precise control of the twisting and winding geometries beyond what is possible in practice. And at the end of one layer, the wire moves to the next layer over some finite distance, so the staircase function for the field is only an approximation.

A better way to use the stepped-field approximation is to find the worst-case situation within a reasonable tolerance of the design. Given the periodic nulls and maxima in the loss as a function of pitch, the solution of interest for design is the set of those peaks, rather than the nulls. Each peak corresponds to linking a half-pitch worth of flux. As the pitch gets shorter, this is less flux in this scenario, and the bundle-level proximity effect loss is reduced. However, the dc resistance and the strand-level proximity effect loss increase with shorter pitch. This tradeoff will be illustrated in a design example.

A. Design Examples

A design example similar to the example in [17] was chosen: a 30-turn winding on an EC-70 size ferrite core, with an 8 A rms, 150 kHz sinusoidal current in the winding. One of the designs in [3] uses 1050 strands of AWG 44 (50 μm diameter) wire. The construction of this wire was not specified in [17], but we can use the guidance in [12] to find a maximum number of strands for the first twisting step,

$$n_{1,max} = 4\frac{\delta^2}{d^2} \tag{20}$$

which indicates we should have a maximum of 48 strands combined in the first step. We also wish to avoid combining more than 5 sub-bundles in subsequent steps. A construction that satisfies these criteria and provides 1050 strands in total is $5 \times 5 \times 42$. This was modeled using the implementation described in Section V, for a range of pitches.

As expected, the pitch of the final twisting operation was found to be the most critical. Fig. 7 shows the total predicted power loss for a range of values for this pitch, with a pitch of 9 mm for the first operation and 15.1 mm for the second operation with the direction of twisting alternating between layers. We see that the region near a 35 mm pitch is generally a good choice; for shorter pitches the losses trend up because on the increased resistance from longer path lengths, whereas for longer pitches the peaks in loss at specific pitches caused by bundle-level proximity effect get worse. In theory, it would be possible to use a long pitch carefully tuned to one of the valleys in this plot, but tuning the pitch that precisely is unlikely to be practical, and it is better to design based on the envelope of the peaks.

In practice, a pitch of 35 mm could be specified. This is near typical values used in practice, so it does not indicate a need to change from current practice. However, this result is specific to this design and is not a general conclusion. For examining this example in more detail, we used a pitch of 36.258 mm, a value chosen to fall on a local peak near 35 mm, to represent the worst case for a nominal value of 35 mm. The value for pitch of the intermediate level of twisting was similarly chosen at a peak. For these pitch values, the loss breakdown in shown in Table I. The majority of the loss is simply $I_{rms}^2 R_{dc}$, with the strand-level proximity effect loss also contributing a substantial 31% of the loss. These are the two effects that are modeled explicitly in most prior work, and this result confirms the validity of that approach. The bundle-level effects have only a minor effect, with bundle-level skin effect increasing the lossy only 1.1% and bundle-level proximity effect contributing only 1.4%. This confirms

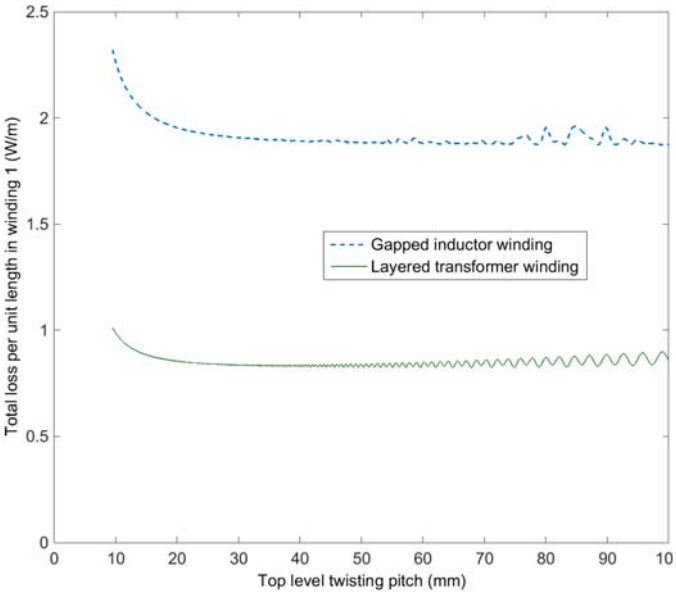

Fig. 7. Total litz wire power losses per unit length for the example winding with 30 turns on an EC70 ferrite core as a function of the pitch of the final twisting step in the litz wire construction. The transformer curve is for one winding in a transformer with layered windings; the inductor curve is for an inductor with a gapped centerpost in the core.

that the value given in (20 for the maximum recommended number of strands combined in the first twisting operation, n_1, is a good choice—it keeps the bundle-level skin effect low while avoiding excessive complexity.

In a gapped inductor, it may be more difficult to cancel out flux linked at the bundle level through twisting, because the flux is highly localized near the gap. To examine this we also examined the same winding on the same core, but as an inductor with a gap in the centerpost of the core. A simple 2-D finite element analysis in the plane parallel to the core was used to find a vector value of H for each turn of the winding, by evaluating the value in the center of the turn. The field along the length of the winding was estimated by linearly interpolating between these values. Although the accuracy of this approach is limited, it serves well to illustrate the differences that can be expected in a gapped inductor winding. Fig. 7 compares the results of this analysis to the transformer results across the same range of pitches. The overall losses are more than doubled, but this is primarily a result of higher

TABLE I
LITZ WIRE LOSSES FOR THE EXAMPLE TRANSFORMER DESCRIBED IN THE TEXT WITH 30 TURNS ON AN EC70 FERRITE CORE.

Loss type	Loss	% of total
DC resistance	1.624 W	66.5%
Skin effect	1.651 W	67.6%
Strand-level proximity effect	0.758 W	31.0%
Bundle-level proximity effect	0.0335 W	1.4%
Increase in dc resistance from twisting	2.8% of R_{dc}	1.9% of total loss

TABLE II
LITZ WIRE LOSSES FOR THE 30-TURN EC-70 GAPPED INDUCTOR DESCRIBED IN THE TEXT.

Loss type	Loss	% of total
DC resistance	1.624 W	29.3%
Skin effect	1.651 W	29.8%
Strand-level proximity effect	3.88 W	69.9%
Bundle-level proximity effect	0.015 W	0.28%
Increase in dc resistance from twisting	2.9% of R_{dc}	0.84% of total loss

strand-level proximity-effect losses in the high-field region near the gap, not a result of bundle-level losses. The more complex flux pattern does result in a more complex pattern of losses as a function of pitch, but the overall trend is similar, and a 35 mm pitch is again a good choice. To evaluate worst-case loss with a pitch near that value, we used a pitch of 37.01 mm, resulting in the loss breakdown shown in Table II.

This example shows that keeping the wire away from the gap should be a high priority, not because of complex bundle level effects, but simply because the strong field causes high strand-level losses. If the winding configuration leaves open a semi-circular ”keep-away” region near the gap, the simple approximation in [12] to estimate losses and choose number and diameter of strands for better performance. An optimization of the shape of the keep-away region, and of the litz wire in conjunction with that shape is developed in [18]–[21], for which software is available for download or to run online at [22]. As the wire is moved away from the gap, the field it is subjected to will be more uniform, and the bundle-level losses will be more similar to those in a transformer.

If the wire is shorter compared to the pitch, the bundle-level effects can be more important. To examine this case, we also consider an example of a PQ20/16 core wound with 6 turns of the same 1050-strand litz wire. The average turn length is 44 mm, slightly less than half that of the first example on the EC70 core, and with fewer turns as well, the overall litz wire length, at 0.264 m, is more than a factor of 10 shorter. The power loss as a function of top-level pitch is shown in Fig. 8. Now we see much more dramatic increases in loss as the pitch gets too long, and the optimal pitch is about 12 mm, a factor of three lower than in the EC70 design. As before we model a worst case for a nominal pitch of 12 mm by finding a nearby peak at a pitch of 12.28 mm, and tabulate the results in Table III. The results are very different from the first case: now, the bundle level proximity effect is as important as the strand-level proximity effect, and the increase in resistance from twisting is also substantial.

The loss per unit length in this example is 22% higher than in the EC-70 example, even with the pitch re-optimized. If the pitch chosen for the EC-70 example were to be used here, the loss would be 73% higher than in the EC-70 example. This results show that in some cases, the choice of pitch and the modeling of bundle-level effects is in fact critical.

Overall, these design example results tend to indicate that

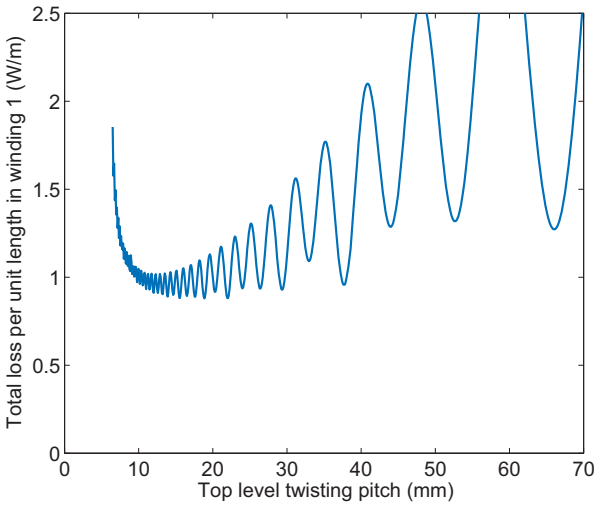

Fig. 8. Total litz wire power losses for a transformer winding with 6 turns on a PQ20/16 ferrite core as a function of the pitch of the final twisting step in the litz wire construction.

when a litz wire is very long compared to the bundle diameter, careful choice of the pitch is not essential, but when the overall length is shorter compared to the diameter, the choice of pitch may be much more important. This criterion typically correlated with the number of turns, as larger numbers of turns typically correspond to both longer length and smaller bundle diameter. Thus, we can conclude that for windings with small numbers of turns, choice of pitch can be critical, and a smaller pitch is needed. Further analysis is needed to more generally identify the situations in which a small pitch is needed, but we tentatively recommend full analysis of designs using less than 20 turns. In those cases, applying the model developed here can help in choosing a good pitch to avoid excessive bundle-level proximity effect losses while also avoiding excessive dc resistance from a shorter-than-necessary pitch. As frequencies used in power electronics increase, more designs require small numbers of turns, especially for low-voltage applications. This will make it increasingly important to model bundle-level effects. Alternatives using foil may also be attractive in these situations [23].

Another important conclusion is that the details of the geometry are important—how sub-bundles pack when they are twisted together affects the overall bundle diameter, which affects the amount of flux linked by bundle-level proximity-effect paths. In the results reported here, we assume that the sub-bundle retain a circular cross section when they are packed together. However, with long pitches in the twisting of sub-bundles, the sub-bundles are not firmly held in shape and can in fact deform as the next twisting step combines them together. Although this was not taken into account in the example calculations we have presented, the calculation method could easily be adapted to account for sub-bundle deformation, given a mechanical model of sub-bundle deformation or given experimental data on bundle and sub-bundle diameters and packing for a specific case.

TABLE III
LITZ WIRE LOSSES FOR THE 6-TURN PQ-CORE TRANSFORMER DESCRIBED IN THE TEXT.

Loss type	Loss	% of total
DC resistance	164 mW	60.86%
Skin effect	166 mW	61.9%
Strand-level proximity effect	57.3 mW	21.3%
Bundle-level proximity effect	45.2 mW	16.8%
Increase in dc resistance from twisting	14.6% of R_{dc}	8.9% of total loss

VIII. Conclusion

This paper has introduced a method of modeling losses in litz wire including the effect of twist at each level of twisting in a multilevel construction. This allows evaluating all the loss effects that are happening in a litz wire in order to determine which are most important, and to determine whether the twisting is adequate to make bundle-level effects negligible. Comparison with a 3-D numerical model shows agreement within the limits of the accuracy of the numerical method and the modeling of the mechanical configuration. Even with some of the intergrals for the new method performed numerically, the computation time is still several orders of magnitude less than a fast numerical solution of the full problem, allowing scans of hundreds of geometries to be completed in a few seconds on a personal computer.

Design examples show that in some cases, typical twisting pitches now used result in good performance with small bundle-level effects and small resistance increases from twisting. However, in cases where the overall litz wire is not sufficiently long compared to its diameter, e.g., for designs with small numbers of turns, the choice of pitch can be critical, with too long a pitch resulting bundle-level proximity effect losses potentially dominating the winding loss. Because small numbers of turns are increasingly common as power electronics switching frequencies increase, analysis of bundle-level effects will be important for many designs. The analysis provided here can serve as a basis for numerical or analytical examination of when these issues are important and for design work in these cases.

References

[1] J. A. Ferreira, "Analytical computation of ac resistance of round and rectangular litz wire windings," *IEE Proceedings-B Electric Power Applications*, vol. 139, no. 1, pp. 21–25, Jan. 1992.

[2] ——, "Improved analytical modeling of conductive losses in magnetic components," *IEEE Trans. on Pow. Electr.*, vol. 9, no. 1, pp. 127–31, Jan. 1994.

[3] C. R. Sullivan, "Optimal choice for number of strands in a litz-wire transformer winding," *IEEE Trans. on Pow. Electr.*, vol. 14, no. 2, pp. 283–291, 1999.

[4] J. Acero, P. J. Hernandez, J. M. Burdío, R. Alonso, and L. Barragdan, "Simple resistance calculation in litz-wire planar windings for induction cooking appliances," *IEEE Trans. on Magnetics*, vol. 41, no. 4, pp. 1280–1288, 2005.

[5] J. Acero, R. Alonso, J. M. Burdio, L. A. Barragan, and D. Puyal, "Frequency-dependent resistance in litz-wire planar windings for domestic induction heating appliances," *IEEE Trans. on Pow. Electr.*, vol. 21, no. 4, pp. 856–866, 2006.

[6] C. Carretero, J. Acero, and R. Alonso, "TM-TE decomposition of power losses in multi-stranded litz-wires used in electronic devices," *Progress In Electromagnetics Research*, vol. 123, pp. 83–103, 2012.

[7] M. Albach, "Two-dimensional calculation of winding losses in transformers," in *IEEE Pow. Electr. Spec. Conf*, vol. 3. IEEE, 2000, pp. 1639–1644.

[8] Xi Nan and C. R. Sullivan, "An equivalent complex permeability model for litz-wire windings," in *Fortieth IEEE Industry Applications Society Annual Meeting*, 2005, pp. 2229–2235.

[9] D. C. Meeker, "An improved continuum skin and proximity effect model for hexagonally packed wires," *Journal of Computational and Applied Mathematics*, vol. 236, no. 18, pp. 4635–4644, 2012.

[10] A. van den Bossche and V. Valchev, *Inductors and Transformers for Power Electronics*. Taylor and Francis Group, 2005.

[11] H. Rossmanith, M. Doebroenti, M. Albach, and D. Exner, "Measurement and characterization of high frequency losses in nonideal litz wires," *IEEE Trans. on Pow. Electr.*, vol. 26, no. 11, pp. 3386–3394, 2011.

[12] C. R. Sullivan and R. Y. Zhang, "Simplified design method for litz wire," in *IEEE Applied Power Electronics Conference and Exposition (APEC)*. IEEE, 2014, pp. 2667–2674.

[13] R. Y. Zhang, C. R. Sullivan, J. K. White, and J. G. Kassakian, "Realistic litz wire characterization using fast numerical simulations," in *IEEE Applied Power Electronics Conference (APEC)*, 2014.

[14] E. C. Snelling, *Soft Ferrites, Properties and Applications*, 2nd ed. Butterworths, 1988.

[15] C. R. Sullivan, "Computationally efficient winding loss calculation with multiple windings, arbitrary waveforms, and two- or three-dimensional field geometry," *IEEE Trans. on Pow. Electr.*, vol. 16, no. 1, pp. 142–50, 2001.

[16] R. Graham, B. Lubachevsky, K. Nurmela, and P. stergrd, "Dense packings of congruent circles in a circle," *Discrete Mathematics*, vol. 181, no. 13, pp. 139–154, 1998. [Online]. Available: http://www.sciencedirect.com/science/article/pii/S0012365X97000502

[17] C. R. Sullivan, "Cost-constrained selection of strand wire and number in a litz-wire transformer winding," *IEEE Trans. on Pow. Electr.*, vol. 16, no. 2, pp. 281–288, Mar. 2001.

[18] J. Hu and C. R. Sullivan, "Optimization of shapes for round-wire high-frequency gapped-inductor windings," in *Proceedings of the 1998 IEEE Industry Applications Society Annual Meeting*, 1998, pp. 900–906.

[19] ——, "Analytical method for generalization of numerically optimized inductor winding shapes," in *IEEE Pow. Electr. Spec. Conf.*, 1999.

[20] C. R. Sullivan, J. McCurdy, and R. Jensen, "Analysis of minimum cost in shape-optimized litz-wire inductor windings," in *IEEE Pow. Electr. Spec. Conf*, 2001.

[21] R. Jensen and C. R. Sullivan, "Optimal core dimensional ratios for minimizing winding loss in high-frequency gapped-inductor windings," in *IEEE Applied Power Electronics Conference*, 2003, pp. 1164 –1169.

[22] "Dartmouth power electronics and magnetic components group web site," http://power.engineering.dartmouth.edu.

[23] C. Sullivan, "Layered foil as an alternative to litz wire: Multiple methods for equal current sharing among layers," in *IEEE Workshop on Control and Modeling for Power Electronics (COMPEL)*, June 2014.